Research Square

Preprints are preliminary reports that have not undergone peer review.
They should not be considered conclusive, used to inform clinical practice,
or referenced by the media as validated information.

Enyne acetogenins from Porcelia macrocarpa fruit peels displayed anti-Trypanosoma cruzi activity in vitro and cause a reduction in the intracellular calcium level in the parasites

Fernanda Thevenard
Universidade Federal do ABC
Ivanildo Brito
Universidade Federal do ABC
Thais Costa-Silva
Serviço Nacional de Aprendizagem Industrial
Andre Tempone
Instituto Adolfo Lutz
Joao Henrique Lago (joao.lago@ufabc.edu.br)
Universidade Federal do ABC

Article

Keywords:

Posted Date: March 20th, 2023

DOI: https://doi.org/10.21203/rs.3.rs-2644250/v1

License: This work is licensed under a Creative Commons Attribution 4.0 International License.
Read Full License

Additional Declarations: No competing interests reported.

Version of Record: A version of this preprint was published at Scientific Reports on June 24th, 2023. See the published version at https://doi.org/10.1038/s41598-023-37520-3.

Abstract

Natural products are a promising source of new compounds with a wide spectrum of pharmacological properties, including antiprotozoal activities. Chagas disease, caused by the protozoan parasite *Trypanosoma cruzi*, is one of several neglected tropical diseases with reduced options for treatment, which presents limitations such as toxicity and ineffectiveness in the chronic stage of the disease. Aiming to investigate the Brazilian flora for the discovery of new anti-*T. cruzi* compounds, the MeOH extract from *Porcelia macrocarpa* R.E. Fries (Annonaceae) fruit peels displayed potent activity against trypomastigotes and intracellular amastigotes and was subjected to bioactivity-guided fractionation. Using different chromatographic steps, it was obtained a fraction composed of a mixture of four new chemically related acetogenins which were characterized as (2*S**,3*R**,4*R**)-3-hydroxy-4-methyl-2-(*n*-octadeca-13',17'-dien-11'-inil)butanolide (**1**), (2*S**,3*R**,4*R**)-3-hydroxy-4-methyl-2-(*n*-eicosa-13',19'-dien-11'-inil)butanolide (**2**), (2*S**,3*R**,4*R**)-3-hydroxy-4-methyl-2-(*n*-octadec-13'-en-11'-inil)butanolide (**3**), and (2*S**,3*R**,4*R**)-3-hydroxy-4-methyl-2-(n-eicosa-13'-en-11'-inil)butanolide (**4**) by analysis of NMR and UHPLC/ESI-HRMS data. The fraction composed of the mixture of compounds **1–4**, displayed an EC_{50} of 4.9 and 2.5 mg/mL against trypomastigote and amastigote forms of *T. cruzi*, respectively, similar to standard drug benznidazole (EC_{50} of 4.8 and 1.4 mg/mL). Additionally, the fraction composed of **1–4** displayed no mammalian toxicity for murine fibroblasts (CC_{50} > 200 mg/mL), resulting in a SI > 40.8 and > 83.3 against trypomastigotes and amastigotes, respectively. Based on these results, the mechanism of action of this fraction was investigated. After a short-time incubation with the trypomastigotes, no alterations in the cell membrane permeability were observed. However, it was verified a decrease in the intracellular calcium of the parasites, without significant pH variations of the acidocalcisomes. The intracellular damages were followed by an upregulation of the reactive oxygen species (ROS) and ATP, but no depolarization effects were observed in the mitochondrial membrane potential. These data suggest that the fraction composed of **1–4** caused an irreversible oxidative stress in the parasites, leading to death. If adequately studied, these acetogenins can open new insights for discovery of new routes of death in *T. cruzi*.

Introduction

Chagas disease (CD) is a disease caused by the protozoan parasite *Trypanosoma cruzi* [1,2] . Transmitted through some reduviid hematophagous insects, CD is endemic to South and Central America, with vector-borne and oral as primary forms of transmission in these regions [3] . Due to globalization and human migration, the incidence of this disease increased in urban centers and in non-endemic countries where the principal transmission form is congenital or vertical transmission [4–7] . This disease presents two clinical phases: an acute phase, mostly asymptomatic and with a high blood parasitemia caused by the trypomastigote forms. The chronic phase is characterized by the presence of intracellular amastigotes and 30% of cases can progress to heart/digestive tract mega-syndromes and is the major cause of cardiac diseases in endemic areas [3, 8–10] . Infecting more than seven million people worldwide, an estimated seven million are affected in Latin America where being about one million women of

reproductive age [1,10] . It is assumed that CD causes about US$ 7 billion/year in production loss, cardiovascular disease treatment, and health care worldwide within US$ 1 billion only in South America [5,6] . Due to a low investment, there are only two drugs available for the clinical treatment, benznidazole and nifurtimox, with efficacy restricted to the acute phase and intense side effects [10,11] . Since cardiac and gastro-intestinal patients are especially susceptive to COVID-19 complications, the outbreak increases the urgency for new drugs and treatments, especially due to impacted health services, and worsening prognostics [12–15] .

In this context, natural products are an alternative in the prospection of new drug prototypes[16]. Previous studies from our research group with *Porcelia macrocarpa* R.E. Fries (Annonaceae) led to metabolites with *in vitro* potential against trypomastigote and amastigote forms of *T. cruzi*. As reported[17,18], extracts from seeds and flowers afforded acetylene acetogenins and fatty acids with potent activity against trypomastigotes forms of *T. cruzi* caused by depolarization of both the plasma membrane and mitochondrial membrane potential of the parasite. As part of our continuous studies with this plant, the MeOH extract from fruits peels of *P. macrocarpa* was prepared and the effect against trypomastigotes and amastigotes of *T. cruzi* was investigated. As a result, it was observed that this extract caused 100% of parasite death at 300 mg/mL indicating the presence of bioactive metabolites. Using a bioactivity-guided approach, it was obtained a fraction composed of a mixture of four new enyne acetogenins (**1–4**) which were chemically characterized by NMR and UHPLC/ESI-HRMS and evaluated against *T. cruzi* trypomastigotes and amastigotes. Finally, insight into the mechanism of lethal action of compounds **1–4** was investigated.

Results And Discussion

Chemical characterization of compounds 1–4. Bioactive fraction (D-1) obtained by chromatographic fractionation of MeOH extract from *P. macrocarpa* (see Methodology) fruit peels was analyzed by UHPLC/UV analysis. As could be seen in Fig. 1, this fraction showed to be composed of four related compounds due to the absorptions at l_{max} at 212, 267 and 283 nm. According with literature data,[19] this profile is characteristic of enyne conjugated system. Molecular formulas for these compounds were established as $C_{23}H_{36}O_3$ (**1**, $[M + H]^+$ and $[M + Na]^+$ at *m/z* 361.2740 and 383.2560), $C_{25}H_{40}O_3$, (**2**, $[M + H]^+$ and $[M + Na]^+$ at *m/z* 389.3054 and 411.2877), $C_{23}H_{38}O_3$, (**3**, $[M + H]^+$ and $[M + Na]^+$ at *m/z* 363.2893 and 385.2722) and $C_{25}H_{42}O_3$, (**4**, $[M + H]^+$ and $[M + Na]^+$ at *m/z* 391.3210 and 413.3034) by ESI-HRMS (Fig. 1). ^{1}H NMR spectra of mixture of compounds **1–4** displayed characteristic signals of a g-lactone ring at δ_H 1.43 (d, *J* = 6.5 Hz, H-5), 2.58 (dt, *J* = 4.8 e 3.0 Hz, H-2), 4.31 (dd, *J* = 4.8 e 3.0 Hz, H-3), and 4.46 (dq, *J* = 6.5 e 3.0 Hz, H-4).[18,19] Signals attributed to hydrogens of a terminal double bond of a alkyl side chain at δ_H 5.82 (ddt, *J* = 16.9, 9.9 e 6.8 Hz, H-19' for **2** and H-17' for **1**) and 4.97 (m, H-20' for **2** and H-18' for **1**) were observed. However, the presence of a triplet at δ_H 0.88 (*J* = 6.9 Hz, H-20' for **4** and H-18´ for **3**), assigned to a terminal methyl group, suggested the presence of related derivatives but containing a sp^3 carbon at terminal position of side chain, similar of related g-lactones isolated from seeds of *P. macrocarpa*.[20]

Interestingly, ^{1}H NMR spectrum showed additional signals at δ_H 6.04 (dt, *J* = 10.7 e 7.6 Hz) and δ_H 5.48 (t, *J* = 10.7 Hz) attributed, respectively, to hydrogens of an enyne conjugation system, in agreement with data obtained from UV spectrum.[20] ^{13}C and DEPT NMR spectra confirmed this proposal, with signals referring to the g-lactone ring at δ_C 177.5 (C-1), 47.6 (C-2), 71.3 (C-3), 78.7 (C-4), and 13.7 (H-5). Signals at δ_C 80.1 and 80.2 were attributed, respectively, to sp carbons C-13' and C-14' whereas those at δ_C 137.6 and 115.2 were assigned to sp^2 carbons in Z configuration – C-16' and C-15', respectively – in order to confirm the presence of enyne system. Furthermore, signals at δ_C 139.2 (C-19' for **2** and C-17' for **1**) and 114.5 (C-20' for **4** and C-18' for **3**), attributed to the terminal double bonds, were also observed. Additionally, these spectra showed a signal at δ_C 14.1 (C-20' for **4** and C-18' for **3**) confirming the presence of derivatives containing terminal methyl group. The positioning of conjugated triple and double bonds on the alkyl side chain for compounds **1–4** was determined at C-11' and C-13', respectively, through MS/MS analysis which exhibited fragments of C-10'/C11' at *m/z* 255.1957 and of C-15'/C-16' at *m/z* 319.2270, as showed in Fig. 1. Finally, the relative configuration of g-lactone ring was determined as *cis,cis,cis* based on values of chemical shifts to carbons C-1, C-2, C-3 and C-4, as observed for chemically related other acetogenins obtained from seeds of *P. macrocarpa*.[20] Therefore, structures of new compounds **1–4** were elucidated as (2*S**,3*R**,4*R**)-3-hydroxy-4-methyl-2-(*n*-octadeca-13',17'-dien-11'-inil)butanolide (**1**), (2*S**,3*R**,4*R**)-3-hydroxy-4-methyl-2-(*n*-eicosa-13',19'-dien-11'-inil)butanolide (**2**), (2*S**,3*R**,4*R**)-3-hydroxy-4-methyl-2-(*n*-octadec-13'-en-11'-inil)butanolide (**3**), and (2*S**,3R*,4*R**)-3-hydroxy-4-methyl-2-(*n*-eicosa-13'-en-11'-inil)butanolide (**4**).

Anti- T. cruzi **activity.** The fraction composed of **1–4** displayed EC_{50} values of 4.9 and 2.5 µg/mL against trypomastigotes and intracellular amastigotes, respectively (Table 1), similar to the values obtained for the standard drug, benznidazole (EC_{50} = 4.8 and 1.4 µg/mL, respectively). No cytotoxicity was observed against mammalian NCTC cells to the highest tested concentration (CC_{50} > 200 µg/mL). The mixture of compounds **1–4** showed elevated selectivity indexes for the bloodstream form (SI > 40.8) and for the intracellular form (SI > 83.3) of the parasite. Comparatively, the standard drug benznidazole resulted in SI > 10.8 for trypomastigotes and > 36.4 for amastigotes. Previous studies[18] evaluated the effect of related acetogenins from seeds of *P. macrocarpa* and compounds with same g-lactone unity, but containing a side chain with a triple bond at C-11' and one double bond at C-19' displayed moderate activity against amastigotes. Otherwise, no effects against *T. cruzi* were observed when a saturated side chain was present, indicating that unsaturation is a crucial feature for the antiparasitic activity. As observed in this work, the effect of the mixture of acetogenins **1–4** against *T. cruzi* was quite similar to the standard drug benznidazole. This data demonstrates that the presence of the enyne conjugated system plays an important role in the potential against the parasite. Therefore, due to the high activity and improvement of SI when compared to benznidazole, the fraction containing compounds **1–4** was subjected to further biological studies to evaluate its mechanism of action against trypomastigotes of *T. cruzi*.

Table 1
Anti-*T. cruzi* activity and cytotoxicity of mixture of acetogenins **1–4** from *P. macrocarpa* fruit peels.

Compounds	[a]EC_{50} (µg/mL)		[b]CC_{50} (µg/mL)	[c]SI	
	trypomastigotes	amastigotes	NCTC	trypomastigotes	amastigotes
1–4	4.9 ± 0.8	2.5 ± 1.0	> 200	> 40.8	> 83.3
Benznidazole	4.8 ± 1.1	1.4 ± 0.6	> 52.0	> 10.8	> 36.4

[a]EC_{50}, 50% effective concentration; [b]CC_{50}, 50% cytotoxic concentration; [c]SI, selectivity index (CC_{50} mammalian cells/EC_{50} parasite form)

Mechanisms of action studies. The lethal mechanisms of the fraction containing compounds **1–4** was performed to evaluate the plasma membrane permeability, the analysis of intracellular calcium levels, the acidocalcisome alkalinization and mitochondrial membrane alterations, including the electric potential, reactive oxygen species and the ATP levels.

Plasma membrane permeability. The plasma membrane regulates transport of ions and nutrients as well as pH and other factors.[21] As such, alterations in its composition can modify the fluidity and contribute to trypomastigote death.[22] Amphotericin B, a clinical drug used in the treatment of *Leishmania* spp., causes permeabilization of the plasma membrane of this protozoan parasite.[23] To evaluate this effect we incubated the fraction with trypomastigotes for a short period and detected alterations in the fluorescence levels using Sytox Green, a fluorescent probe that binds to nucleic acids and increases the fluorescence after membrane damages.[24] Triton X-100, a non-ionic detergent, was used as a positive control to induce the solubilization of the lipid bilayer.[25] No increases in fluorescence levels were observed after treatment with the mixture of compounds **1–4** (Fig. 2), suggesting no effect of the mixture of **1–4** in the membrane of the parasite.

Intracellular Ca^{2+} levels. Calcium ions regulate several signalization pathways, parasite differentiation, flagellar function and are essential for trypanosomatids survival. Alteration of calcium homeostasis can result in the parasite death.[26,27] Using the fluorescent probe Fluo-4AM dye, it was observed that the mixture of **1–4** caused reduction of cytosolic Ca^{2+} levels at all evaluated times of the incubation (Fig. 3), suggesting a metabolic imbalance. To evaluate the intracellular calcium, a known organelle in trypanosomatids was studied, named acidocalcisomes.

Acidocalcisome alkalinization. Acidocalcisomes are acidic organelles and the main Ca^{2+} storage for trypanosomatids, where the ion is bound to polyphosphates.[27,28] The alkalinization of these organelles has been related to leakage of calcium to the cytoplasm.[26] No effect was observed after treatment with the mixture of **1–4** (Fig. 4), corroborating the reduction of calcium levels in the cytoplasm as previously observed. The decrease of the calcium levels may be ascribed to a possible uptake of this ion by the

mitochondria or even though by the endoplasmic reticulum.[27,28] Considering that an elevated concentration of calcium can harm the mitochondria,[29] the electric potential of this vital organelle was investigated.

Mitochondrial membrane potential (Δψm). The single mitochondrion is unique to the trypanosomatids and is essential for the bioenergetic metabolism. It is also involved in calcium homeostasis as a known source of reactive oxygen species (ROS). Due to these characteristics, the *T. cruzi* mitochondria has been considered an interesting target for new anti-trypanosomal drugs.[29,30] Compounds that affect the respiratory chain tend to impact the ROS production and can also induce oxidative stress. Using the JC-1 probe, alterations in the mitochondrial membrane potential were evaluated. As result, no decreases of the fluorescence levels were detected after treatment with the mixture of **1–4** (Fig. 5), when compared to untreated parasites. This data reflects no direct impact of the compounds to the organelle. It has been shown that the overloading of calcium by the mitochondria can affect the mitochondrial membrane potential[31], but this effect was not observed after treatment with the mixture of **1–4**. Although no electric alterations were detected in the mitochondria, alterations of reactive oxygen species levels were studied.

ROS. Using the fluorescent probe H_2DCFDA, a significant increase in ROS levels after 2 h of incubation was observed (Fig. 6). Elevation of ROS in trypanosomatids, if not rapidly detoxified by thiols and trypanothione reductase, can induce cell death by a known effect named oxidative stress.[32] Due to this effect, was investigated the energetic metabolism of the parasites, detecting the ATP levels after treatment.

ATP levels. Using a luminescent assay with luciferin, the levels of ATP in the trypomastigotes was quantified. The mixture of **1–4** caused a significant increase in ATP levels (Fig. 7) when compared to untreated cells. This fact may be ascribed to the oxidative stress, resulting in a higher metabolism rate to cope with the damages induced by excessive ROS in the intracellular milieu.

Conclusions

One fraction composed of four new chemically related acetogenins **1–4** was obtained from the MeOH extract of *P. macrocarpa* fruit peels and displayed an anti-trypanosomal activity with similar effect to the standard drug benznidazole. Besides the effect against both clinical forms of the parasite, these new compounds showed no mammalian cytotoxicity, demonstrating a promising potential. Due to this activity, mechanism of action studies were performed. The fraction containing compounds **1–4** reduced the cytosolic calcium levels, with no alkalinization of the acidocalcisomes. Although it induced no depolarization of the mitochondrial membrane potential, increased levels of ATP were detected, as a possible cellular effect to counterbalance the oxidative stress caused by the elevated ROS levels leading to the parasite death.

Methodology

General experimental procedures. Silica gel 60 PF_{254} (Merck - Darmstadt, Germany) was used for thin layer chromatography (TLC) whereas column chromatography (CC) procedures was performed using silica gel 60 (Merck - Darmstadt, Germany) or Sephadex LH-20 (Sigma-Aldrich – St. Louis, MO, USA). NMR spectra were obtained on a Varian Unity INOVA (500 MHz ^{1}H and 125 MHz ^{13}C) using $CDCl_3$ as solvent and TMS as internal standard. Chemical shifts (δ) are given in ppm with coupling constants (*J*) in Hz. UHPLC experiments were performed on a Thermoscientific Ultimate 3000 model with DAD detector (UVD-170 model) and separation was performed on a Kinetex® C_{18} analytic column (5 µm – 250 x 4.6 mm) using ACN:H_2O 85:15 as eluent at 1.0 mL/min. ESI-HRMS were measured on a Bruker Daltonics MicroTOF QII operating with electrospray ionization (positive mode).

Plant material. Fruits of *P. macrocarpa* were collected at the *Instituto de Botânica* in São Paulo city, São Paulo State, Brazil (23º38'33.8"S and 46º37'17.5"W) in 2017. Dr. Maria Claudia M. Young identified the plant material, and a voucher specimen was compared with that under number SP76791. This study was registered on the National System for the Management of Genetic Heritage and Associated Traditional Knowledge (SisGen) from the Ministry of the Environment, Brazil, under code A483B45. Experimental research and field studies on plants (either cultivated or wild), including the collection of plant material have complied with relevant institutional, national, and international guidelines and legislation.

Extraction and bioactivity-guided fractionation. The fruit peels were removed immediately after collection and dried at room temperature. After milling, the plant material (168 g) was defatted (10 X 1L) with *n*-hexane. The residual material was then extracted with MeOH (8 X 1L) at room temperature. After elimination of the solvent under reduced pressure, was obtained the MeOH extract (35 g) which was successively partitioned using *n*-hexane and EtOAc. As both crude MeOH extract and *n*-hexane phase displayed activity against *T. cruzi* (100% of parasite death at 300 mg/mL), part of the *n*-hexane phase (5 g) was fractioned over SiO_2 column chromatography eluted with increasing amounts of EtOAc in hexane to afford 10 fractions (A - J). Bioactive fraction D (1 g) was chromatographed over Sephadex LH-20 eluted with *n*-hexane:CH_2Cl_2 (1:4), CH_2Cl_2:acetone (3:2 and 1:4) to afford eight groups (D-1 to D-8). Fraction D-1 (18 mg) displayed activity against *T. cruzi* and showed to be composed of a mixture of **1–4**.

Bioassay procedures

Animals. BALB/c mice were utilized for *T. cruzi* maintenance infection and peritoneal macrophage collection.[33] The mice were obtained from the animal breeding facility at the *Instituto Adolfo Lutz* – São Paulo, Brazil and maintained in sterilized boxes with absorbent material under a controlled environment. Food and water were given *ad libitum*. Procedures were approved by the Ethics Committee of the *Instituto Adolfo Lutz* (Project CEUA-IAL/Pasteur05/2018), in agreement with the Guide for the Care and Use of Laboratory Animals from the National Academy of Sciences.

Parasite and mammalian cell maintenance. Trypomastigotes (Y strain) were maintained in rhesus monkey kidney cells (LLC-MK2 – ATCC CCL 7) using RPMI-1640 medium supplemented with 2% bovine

fetal serum (BFS) in an incubator humidified with 5% CO_2 at 37°C. LLC-MK2 and conjunctive mice cells (NCTC clone L929, ATCC) were maintained at 37°C with RPMI-1640 supplemented with 10% BFS at 5% CO_2. Macrophages were obtained from the peritoneal cavities of BALB/c mice through washing with the same medium.[34,35]

In vitro *activity against trypomastigote forms of* T. cruzi. Trypomastigotes were obtained from previously infected LLC-MK2 cultures and counted in a Neubauer hemocytometer seeded at 1 x 10^6 cells/well (96 well plates). The mixture of compounds **1–4** was added in serial dilution (100–1.6 mg/mL) using RPMI-1640 medium and the plated were incubated for 24 h at 37°C in a 5% CO_2-humidified incubator. Benznidazole was used as the standard drug. Trypomastigote viability was evaluated by the resazurin assay.[17,34]

In vitro *activity against amastigote forms of* T. cruzi. Previously obtained macrophages were plated on 16 well chamber slides (NUNC®, Merck) at 1 x 10^5 macrophage/well and incubated for 24 h at 37°C in a 5% CO_2-humidified incubator. Trypomastigotes were washed with RPMI-1640 medium and used to infect the cells at 1 x 10^6/well for 2 h. After this time, non-internalized parasites were removed by washing with RPMI-1640 medium. Serial dilutions of the mixture of compounds **1–4** (100–1.6 mg/mL) were incubated with infected macrophages for 48 h at 37°C and 5% CO_2 with benznidazole as the standard drug. Slides were then fixed with MeOH and stained with Giemsa. EC_{50} values were obtained after counting infected cells with an light microscope (EVOS M5000) and calculated according to literature.[33,35]

Cytotoxicity against mammalian cells and selectivity index determination. Cytotoxicity was evaluated against NCTC cells (L929 clone). Cells were incubated at 6 x10^4/well with serial dilutions (200–1.6 mg/mL) of active fractions in RPMI medium supplemented with 10% BFS (48 h, 37°C, 5% CO_2). CC_{50} values were obtained by MTT assay. Optical density was determined by fluorimetric microplate reader (FilterMax F5, MolecularDevices) at a wavelength of 570 nm.[33] Selectivity indexes (SI) for both forms of *T. cruzi* were calculated using the ratio - SI = CC_{50} against NCTC cells/EC_{50} against parasite forms.

Mechanism of action studies

SYTOX Green assay for cell membrane permeability. Washed trypomastigotes (2 x 10^6/well) were incubated with 1 µM SYTOX Green probe (Molecular Probes) in HANKS' balanced salt solution (HBSS, Sigma-Aldrich) supplemented with 10 mM D-Glucose in the dark. A mixture of compounds **1–4** was added (t = 0 min) and fluorescence levels were measured every 20 min for 120 min. Untreated parasites were the negative control and maximum permeabilization was achieved with 0.5% Triton X-100. Fluorescence intensity was determined by fluorometric microplate reader (FilterMax F5) with excitation and emission wavelengths of 485 and 520 nm, respectively. Triton X-100 was added to all samples at the end of the assay.

Measurement of intracellular calcium (Ca^{2+}) levels. Trypomastigotes (2 x 10^6/well) were pre-treated with Fluo-4AM dye (5 μM) in Phosphate Buffer Solution (PBS) at 37°C in the dark, for 1 h. Parasites were then briefly washed and treated with the mixture of compounds **1–4** at EC_{50} value. Using a fluorometric microplate reader (FilterMax F5 Multi-mode, Molecular Devices), fluorescence levels were measured for 260 min (485 and 535 nm for excitation and emission wavelengths, respectively). Negative control consisted of untreated parasites and maximum intracellular calcium levels were obtained using 0.5% Triton X-100 (v/v). [36,37]

Alterations in acidocalcisomes. Trypomastigotes (2 x 10^6/well in 96 well plates) were washed with PBS and incubated with acridine orange dye (Thermo Fisher Scientific) at 4 μM for 5 min in the dark. Non-internalized probe was removed with PBS. The mixture of compounds **1–4** was incubated with the parasite at CE_{50} concentration for 140 min. Fluorescence levels were measured using Multimode FilterMax F5 (Molecular Devices) microplate reader with excitation and emission wavelengths of 485 and 535 nm, respectively. Nigericin (4 μM) was used as positive control and non-treated parasites as negative control.[37]

Mitochondrial membrane potential (Δψm). Trypomastigotes (2 x 10^6/tube) were washed with HBSS supplemented with NaHCO3 and D-glucose and incubated with the mixture of compounds **1–4** (EC_{50} value) at 37°C and 5% CO_2 for 1 and 2 h. After washing, JC-1 dye (10 μM) was added and the parasites were incubated for 20 min at 37°C in the dark. Fluorescence was measured in a Attune NxTflow cytometer (488 and 530/574 nm excitation and emission wavelengths, respectively). The mitochondrial membrane potential was determined by the ratio between red/green fluorescence intensities (BL-2/BL-1). Positive and negative control were CCCP (Sigma-Aldrich) at 100 μM and non-treated parasites, respectively.[37]

Measurement of ROS levels. The mixture of compounds **1–4** was incubated with washed trypomastigotes (2 x 10^6/well) in black 96 well plates in HBSS supplemented with $NaHCO_3$ (4.2 mM) and D-glucose (10 mM), at EC_{50} value for 1 and 2 h (24°C, 5% CO_2). Azide (10 μM) and untreated parasites were used as positive and negative controls, respectively. Afterwards, H_2DCFDA (20 μM) was incubated with the parasites for 15 min at 37°C. Fluorescence intensity was measured using FilterMax F5 microplate reader (485 and 520 nm excitation and emission wavelengths, respectively). Controls containing only the compound and the fluorophore were added in all experiments to measure interference.[38,39]

Measurement of ATP levels. The mixture of compounds **1–4** at EC_{50} value was incubated with trypomastigotes (2 x 106/well) in HBSS and glucose for 1 and 3 h, at 37°C. Parasites were lysed with 0.5% Triton X-100 and mixed with a standard reaction buffer (ATP Determination kit – Thermo Fisher) containing DTT (1 mM), luciferin (0.5 mM) and luciferase (1.25 μg/mL). A luminometer (FilterMax F5

Multi-mode, Molecular Devices) was used for measuring luminescence intensity and ATP quantity calculated with an ATP standard curve.[37]

Statistical analysis. Samples were tested in duplicates of three independent assays. Calculation of EC_{50} and CC_{50} values was performed using dose-response sigmoid curves in Graph-Pad Prism (GraphPad Prism software 6.0, San Diego, CA, USA). Mechanism of active studies were analyzed using ANOVA turkey test for significance ($p < 0.05$).[36]

Declarations

Acknowledgments

The authors would like to thank São Paulo Research Foundation - FAPESP (Projects 2020/01221-4, 2021/02789-7 and 2021/04464-8), CAPES (financial code 001) and the National Council for Scientific and Technological Development - CNPq (301354/2019-4 and 405691/2021-1) for the financial support. This publication is part of the activities of the Research Network Natural Products against Neglected Diseases (ResNetNPND): http://www.uni-muenster.de/ResNetNPND/.

Author contributions

F.T., I.A.B. and J.H.G.L. contributed to chromatographic procedures and chemical characterization. F.T., T.A.C.S., A.G.T. and J.H.G.L. contributed to the manuscript preparation. T.A.C.S and A.G.T. contributed to the bioactivity tests and mechanism of action studies. All authors read, revised, and approved the manuscript.

Data availability statement

The datasets used and/or analyzed during the current study available from the corresponding author on reasonable request.

Competing interests

The authors declare no competing interests.

References

1. *Chagas disease (also known as American trypanosomiasis)*. https://www.who.int/news-room/fact-sheets/detail/chagas-disease-(american-trypanosomiasis) (accessed 2022-04-09).
2. *Doença de Chagas | DNDi América Latina*. https://www.dndial.org/doencas/doenca-chagas/.
3. Echeverría, L. E.; Marcus, R.; Novick, G.; Sosa-Estani, S.; Ralston, K.; Zaidel, E. J.; Forsyth, C.; Ribeiro, A. L. P.; Mendoza, I.; Falconi, M. L.; Mitelman, J.; Morillo, C. A.; Pereiro, A. C.; Pinazo, M. J.; Salvatella, R.;

Martinez, F.; Perel, P.; Liprandi, Á. S.; Piñeiro, D. J.; Molina, G. R. WHF IASC Roadmap on Chagas Disease. Glob. Heart 2020, *15* (1), 26.

4. Schaub, G. A. An Update on the Knowledge of Parasite–Vector Interactions of Chagas Disease. Res. Rep. Trop. Med. 2021, *12*, 63–76.
5. Lidani, K. C. F.; Andrade, F. A.; Bavia, L.; Damasceno, F. S.; Beltrame, M. H.; Messias-Reason, I. J.; Sandri, T. L. Chagas Disease: From Discovery to a Worldwide Health Problem. Front. Public Health 2019, *7*, 166.
6. Lascano, F.; García Bournissen, F.; Altcheh, J. Review of Pharmacological Options for the Treatment of Chagas Disease. Br. J. Clin. Pharmacol. 2022, *88* (2), 383–402.
7. Abras, A.; Ballart, C.; Fernández-Arévalo, A.; Pinazo, M.-J.; Gascón, J.; Muñoz, C.; Gállego, M. Worldwide Control and Management of Chagas Disease in a New Era of Globalization: A Close Look at Congenital *Trypanosoma cruzi* Infection. Clin. Microbiol. Rev. 2022, *35* (2), e00152-21.
8. Alonso-Padilla, J.; Cortés-Serra, N.; Pinazo, M. J.; Bottazzi, M. E.; Abril, M.; Barreira, F.; Sosa-Estani, S.; Hotez, P. J.; Gascón, J. Strategies to Enhance Access to Diagnosis and Treatment for Chagas Disease Patients in Latin America. Expert Rev. Anti Infect. Ther. 2019, *17* (3), 145–157.
9. García-Huertas, P.; Cardona-Castro, N. Advances in the Treatment of Chagas Disease: Promising New Drugs, Plants and Targets. Biomed. Pharmacother. 2021, *142*, 112020.
10. Soeiro, M. de N. C. Perspectives for a New Drug Candidate for Chagas Disease Therapy. Mem. Inst. Oswaldo Cruz 2022, *117*, e220004.
11. Porrás, A. I.; Yadon, Z. E.; Altcheh, J.; Britto, C.; Chaves, G. C.; Flevaud, L.; Martins-Filho, O. A.; Ribeiro, I.; Schijman, A. G.; Shikanai-Yasuda, M. A.; Sosa-Estani, S.; Stobbaerts, E.; Zicker, F. Target Product Profile (TPP) for Chagas Disease Point-of-Care Diagnosis and Assessment of Response to Treatment. PLoS Negl. Trop. Dis. 2015, *9* (6), e0003697.
12. Ferreira, L. L. G.; Andricopulo, A. D. World Chagas Disease Day and the New Road Map for Neglected Tropical Diseases. Curr. Top. Med. Chem. 2020, *20* (17), 1518.
13. Goldenberg, S. Chagas Disease Treatment: A 120-Year-Old Challenge to Public Health. Mem. Inst. Oswaldo Cruz 2022, *117*, e210501chgsa.
14. Diaz-Hernandez, A.; Gonzalez-Vazquez, M. C.; Arce-Fonseca, M.; Rodriguez-Morales, O.; Cedilllo-Ramirez, M. L.; Carabarin-Lima, A. Risk of COVID-19 in Chagas Disease Patients: What Happen with Cardiac Affectations? *Biology* 2021, *10* (5), 411.
15. Zaidel, E. J.; Forsyth, C. J.; Novick, G.; Marcus, R.; Ribeiro, A. L. P.; Pinazo, M.-J.; Morillo, C. A.; Echeverría, L. E.; Shikanai-Yasuda, M. A.; Buekens, P.; Perel, P.; Meymandi, S. K.; Ralston, K.; Pinto, F.; Sosa-Estani, S. COVID-19: Implications for People with Chagas Disease. Glob. Heart 2020, *15* (1), 69.
16. Newman, D. J.; Cragg, G. M. Natural Products as Sources of New Drugs over the Nearly Four Decades from 01/1981 to 09/2019. J. Nat. Prod. 2020, *83* (3), 770.
17. Londero, V. S.; da Costa-Silva, T. A.; Gomes, K. S.; Ferreira, D. D.; Mesquita, J. T.; Tempone, A. G.; Young, M. C. M.; Jerz, G.; Lago, J. H. G. Acetylenic Fatty Acids from *Porcelia macrocarpa*

(Annonaceae) against Trypomastigotes of *Trypanosoma cruzi*: Effect of Octadec-9-ynoic Acid in Plasma Membrane Electric Potential. Bioorganic Chem. 2018, *78*, 307.

18. Oliveira, E. A.; Brito, I. A.; Lima, M. L.; Romanelli, M.; Moreira-Filho, J. T.; Neves, B. J.; Andrade, C. H.; Sartorelli, P.; Tempone, A. G.; Costa-Silva, T. A.; Lago, J. H. G. Antitrypanosomal Activity of Acetogenins Isolated from the Seeds of *Porcelia macrocarpa* Is Associated with Alterations in Both Plasma Membrane Electric Potential and Mitochondrial Membrane Potential. J. Nat. Prod. 2019, *82* (5), 1177.
19. Bousserouel, H.; Awang, K.; Guéritte, F.; Litaudon, M. Enyne- and Enediyne-γ-Lactones from the Bark of *Meiogyne cylindrocarpa*. Phytochem. Lett. 2012, *5* (1), 29.
20. Roque, N. F., Chaves, M. H. Acetogenins from Porcelia *macrocarpa*: Stereochemical Determination of 2-Alkyl-3-Hydroxyl-4-Methyl-g-Lactones by ^{13}C NMR Spectroscopy. 1997, *44*(3), 523.
21. Tiwari, N.; Gedda, M. R.; Tiwari, V. K.; Singh, S. P.; Singh, R. K. Limitations of Current Therapeutic Options, Possible Drug Targets and Scope of Natural Products in Control of Leishmaniasis. Mini-Rev. Med. Chem. 2017, *18* (1).
22. Alexandre, T. R.; Lima, M. L.; Galuppo, M. K.; Mesquita, J. T.; do Nascimento, M. A.; dos Santos, A. L.; Sartorelli, P.; Pimenta, D. C.; Tempone, A. G. Ergosterol Isolated from the Basidiomycete *Pleurotus salmoneostramineus* Affects *Trypanosoma cruzi* Plasma Membrane and Mitochondria. J. Venom. Anim. Toxins Trop. Dis. 2017, *23* (1), 30.
23. Chattopadhyay, A.; Jafurulla, Md. A Novel Mechanism for an Old Drug: Amphotericin B in the Treatment of Visceral Leishmaniasis. Biochem. Biophys. Res. Commun. 2011, *416* (1–2), 7.
24. Morais, T. R.; Conserva, G. A. A.; Varela, M. T.; Costa-Silva, T. A.; Thevenard, F.; Ponci, V.; Fortuna, A.; Falcão, A. C.; Tempone, A. G.; Fernandes, J. P. S.; Lago, J. H. G. Improving the Drug-Likeness of Inspiring Natural Products - Evaluation of the Antiparasitic Activity against *Trypanosoma cruzi* through Semi-Synthetic and Simplified Analogues of Licarin A. Sci. Rep. 2020, *10* (1), 5467.
25. Koley, D.; Bard, A. J. Triton X-100 Concentration Effects on Membrane Permeability of a Single HeLa Cell by Scanning Electrochemical Microscopy (SECM). *Proc. Natl. Acad. Sci. USA* 2010 *107*(39), 16783.
26. Moreno, S. N.; Docampo, R. Calcium Regulation in Protozoan Parasites. Curr. Opin. Microbiol. 2003, *6* (4), 359.
27. Docampo, R.; Huang, G. Calcium Signaling in Trypanosomatid Parasites. Cell Calcium 2015, *57* (3), 194.
28. Docampo, R.; Moreno, S. N. J. Acidocalcisomes. Cell Calcium 2011, *50* (2), 113.
29. Vannier-Santos, M.; Martiny, A.; Souza, W. Cell Biology of *Leishmania* Spp.: Invading and Evading. Curr. Pharm. Des. 2002, *8* (4), 297.
30. Kaczanowski, S.; Sajid, M.; Reece, S. E. Evolution of Apoptosis-like Programmed Cell Death in Unicellular Protozoan Parasites. Parasit. Vectors 2011, *4* (1), 44.

31. Amaral, M.; Sousa, F. S.; Silva, T. A. C.; Junior, A. J. G.; Taniwaki, N. N.; Johns, D. M.; Lago, J. H. G.; Anderson, E. A.; Tempone, A. G. A Semi-Synthetic Neolignan Derivative from Dihydrodieugenol B Selectively Affects the Bioenergetic System of *Leishmania infantum* and Inhibits Cell Division. Sci. Rep. 2019, *9* (1), 6114.
32. Reimão, J.Q.; Migotto, A.E.; Kossuga, M.H.; Berlinck, R.G.; Tempone, A.G. Antiprotozoan activity of Brazilian marine cnidarian extracts and of a modified steroid from the octocoral *Carijoa riisei*. Parasitol Res. 2008, *103*, 1445.
33. Silva, M. L.; Costa-Silva, T. A.; Antar, G. M.; Tempone, A. G.; Lago, J. H. G. Chemical Constituents from Aerial Parts of *Baccharis sphenophylla* and Effects against Intracellular Forms of *Trypanosoma cruzi*. Chem. Biodiv. 2021, *18*, 10.
34. Galhardo, T. S.; Ueno, A. K.; Costa-Silva, T. A.; Tempone, A. G.; Carvalho, W. A.; Fischmeister, C.; Bruneau, C.; Mandelli, D.; Lago, J. H. G. New Derivatives from Dehydrodieugenol B and Its Methyl Ether Displayed High Anti-*Trypanosoma cruzi* Activity and Cause Depolarization of the Plasma Membrane and Collapse the Mitochondrial Membrane Potential. Chem. Biol. Interact. 2022, *366*, 110129.
35. Londero, V. S.; Costa-Silva, T. A.; Tempone, A. G.; Namiyama, G. M.; Thevenard, F.; Antar, G. M.; Baitello, J. B.; Lago, J. H. G. Anti-*Trypanosoma cruzi* Activity of Costic Acid Isolated from *Nectandra barbellata* (Lauraceae) Is Associated with Alterations in Plasma Membrane Electric and Mitochondrial Membrane Potentials. Bioorg. Chem. 2020, *95*, 103510.
36. Umehara, E.; Costa Silva, T. A.; Mendes, V. M.; Guadagnin, R. C.; Sartorelli, P.; Tempone, A. G.; Lago, J. H. G. Differential Lethal Action of C17:2 and C17:0 Anacardic Acid Derivatives in *Trypanosoma cruzi* – A Mechanistic Study. Bioorganic Chem. 2020, *102*, 104068.
37. Costa-Silva, T. A.; Silva, M. L.; Antar, G. M.; Tempone, A. G.; Lago, J. H. G. *Ent*-Kaurane Diterpenes Isolated from n-Hexane Extract of *Baccharis sphenophylla* by Bioactivity-Guided Fractionation Target the Acidocalcisomes in *Trypanosoma cruzi*. Phytomedicine 2021, *93*, 153748.
38. Mukherjee, S. B.; Das, M.; Sudhandiran, G.; Shaha, C. Increase in Cytosolic Ca^{2+} Levels through the Activation of Non-Selective Cation Channels Induced by Oxidative Stress Causes Mitochondrial Depolarization Leading to Apoptosis-like Death in *Leishmania donovani* Promastigotes. J. Biol. Chem. 2002, *277* (27), 24717.
39. Romanelli, M. M.; Amaral, M.; Thevenard, F.; Cruz, L. M. S.; Regasini, L. O.; Migotto, A. E.; Lago, H. G.; Tempone, A. G. Mitochondrial Imbalance of *Trypanosoma cruzi* Induced by the Marine Alkaloid 6–Bromo-2'-De–*N*–Methylaplysinopsin. ACS Omega 2022, *7*(32), 28561.

Figures

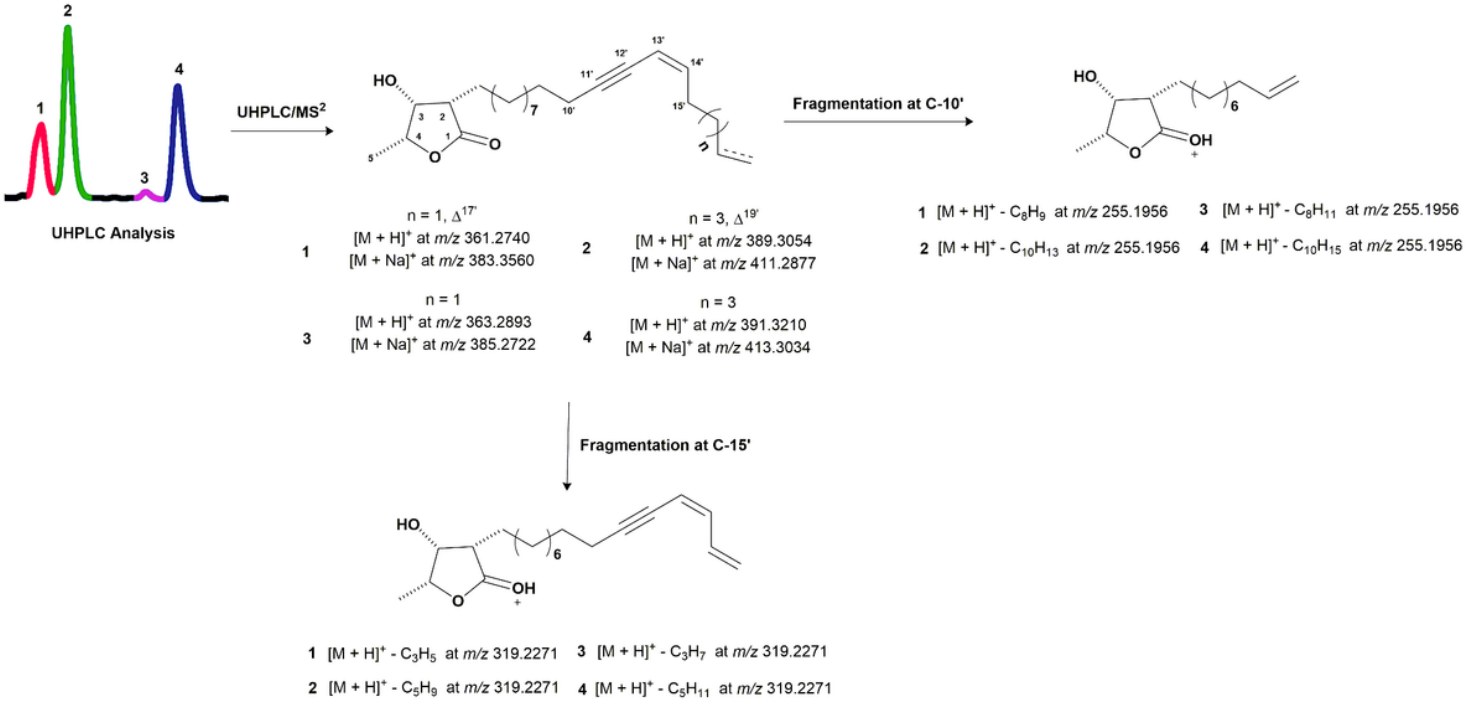


Figure 1

Chemical structures of acetogenins 1 – 4 from P. macrocarpa fruit peels and UHPLC-ESI-HRMS/MS (positive mode) analysis.

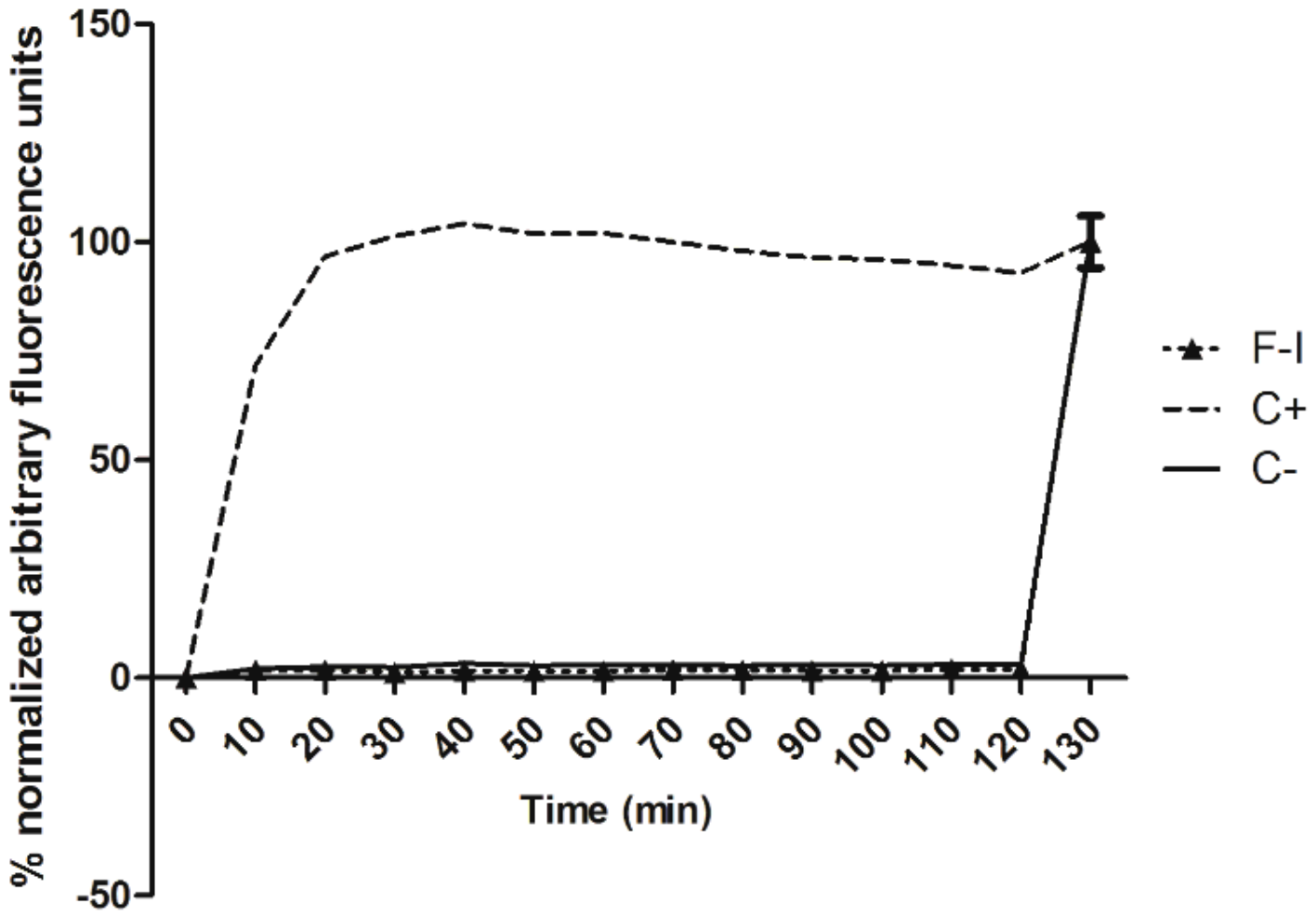


Figure 2

Evaluation of cell membrane permeability effects of the mixture of compounds 1 – 4 from *P. macrocarpa* fruit peels in *T. cruzi* trypomastigotes. Sytox Green dye (excitation and emission wavelengths of 485 and 520 nm) was used, and fluorescence was monitored until 130 minutes. Untreated parasites (C-) and Triton X 100 (C+) were used for minimum and maximum permeabilization, respectively. A representative assay is shown.

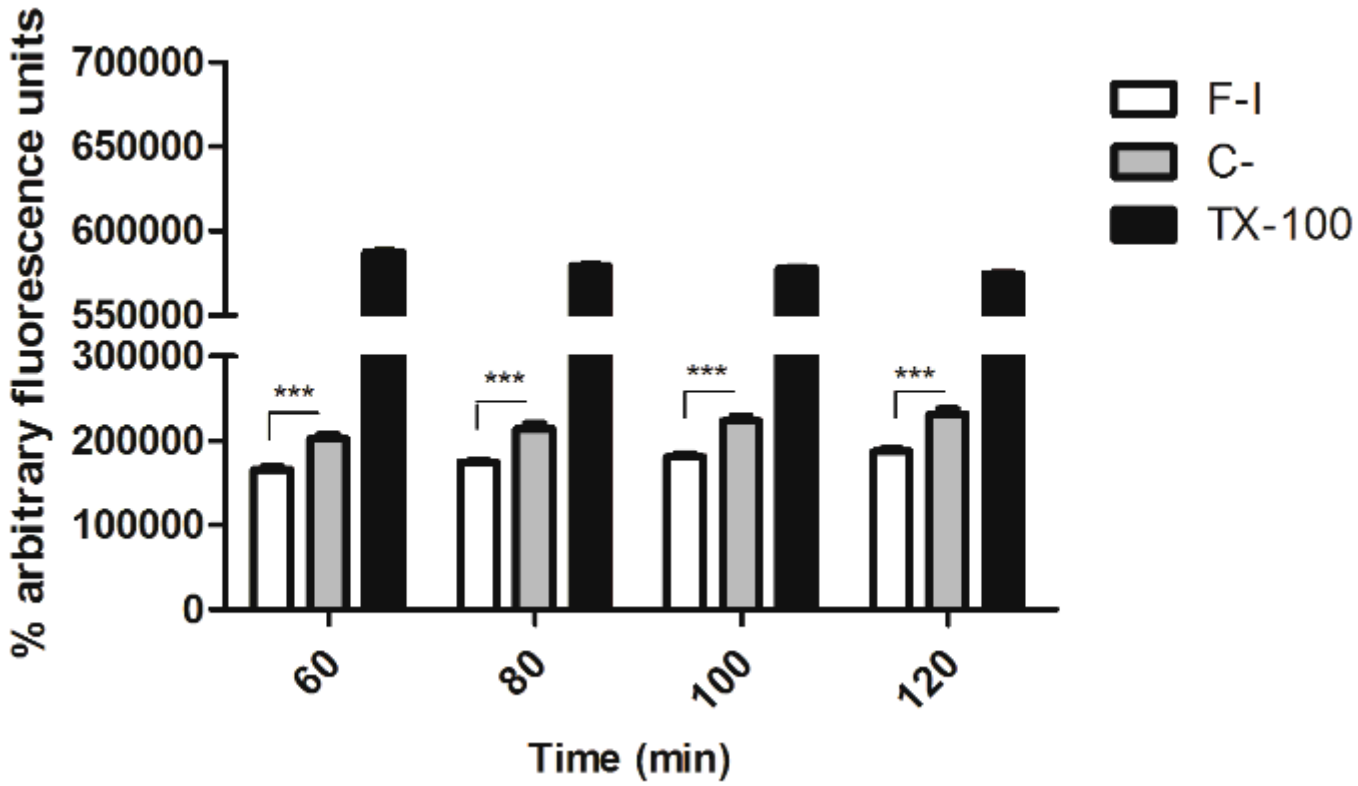


Figure 3

Effect of the mixture of compounds 1 – 4 from *P. macrocarpa* fruit peels on intracellular calcium levels in *T. cruzi* trypomastigotes. Using Fluo-4AM dye (excitation and emission wavelengths of 485 nm and 535, respectively), parasites were treated with I for 60-, 80-, 100- and 120-min. Positive (C+) and negative (C-) controls were Triton X-100 (0.5% v/v) and untreated parasites, respectively, Fluorescence in arbitrary units at each time point. A representative assay is shown. ***p<0.0001.

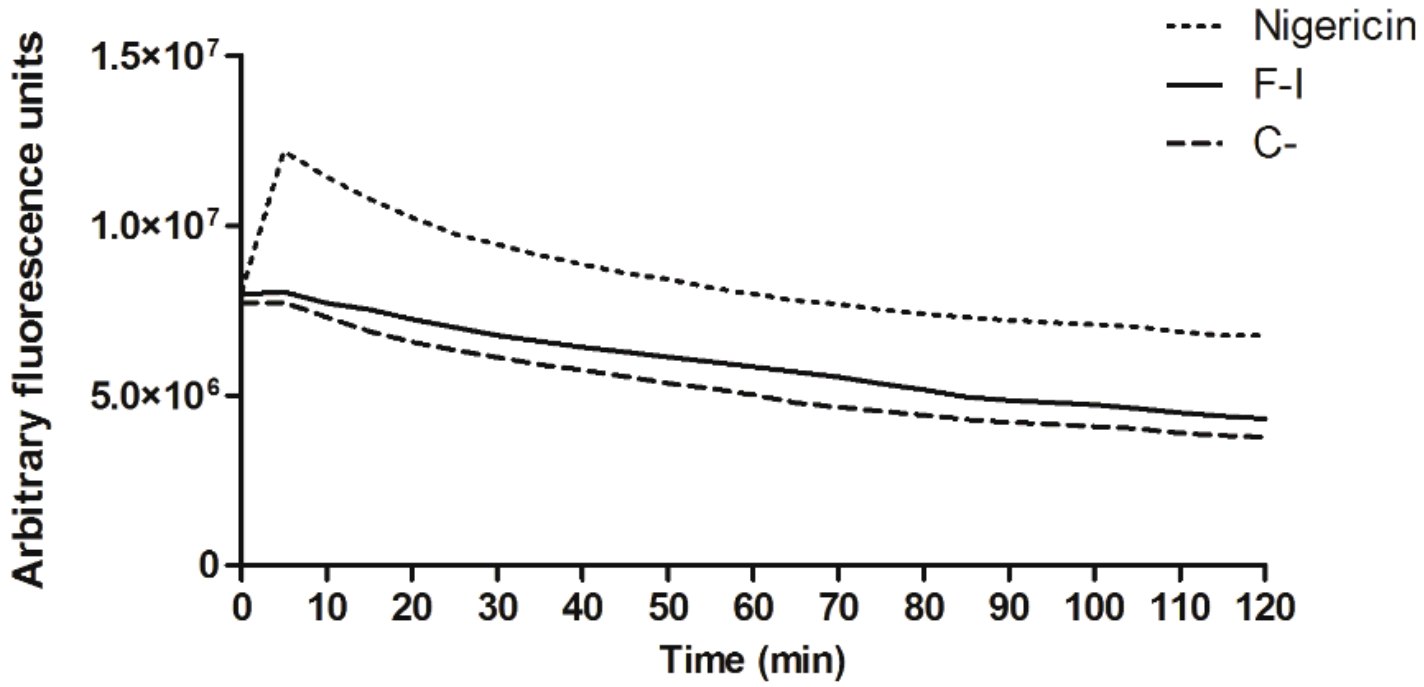


Figure 4

Time dependent analysis of acidocalcisome alkalization of *T. cruzi* trypomastigotes treated with the mixture of compounds 1 – 4 from *P. macrocarpa* fruit peels. Pretreatment with acridine orange dye (4 µM) was performed before treating the parasites with the mixture of compounds **1 – 4** for 120 min. Nigericin (4 µM) and non-treated parasites were the positive (C+), and negative (C-) control, respectively. A representative assay is shown.

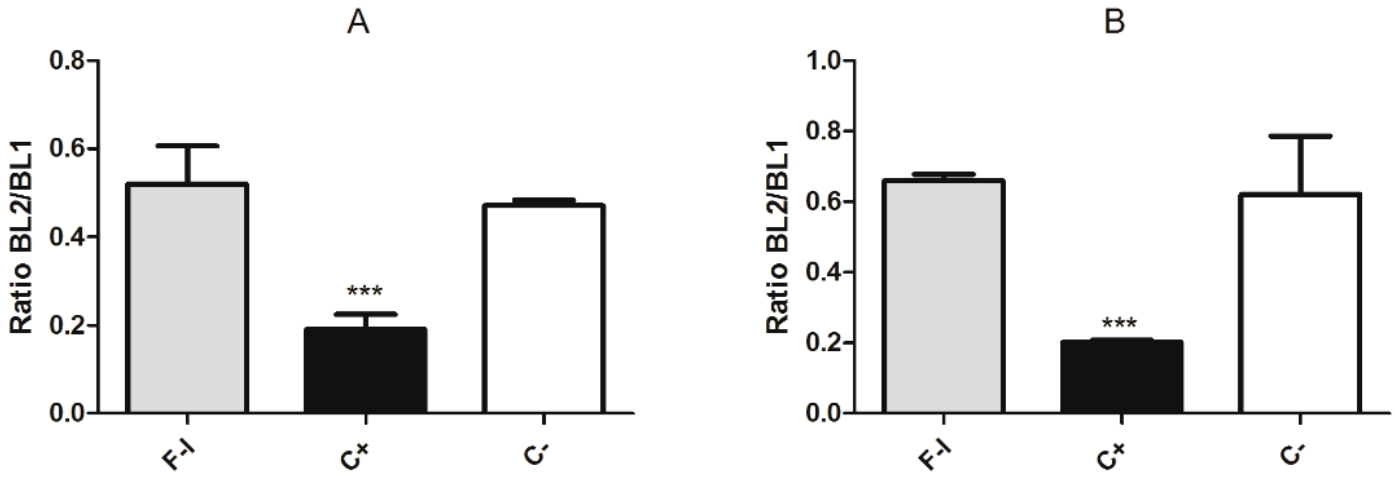


Figure 5

Effect of the mixture of compounds 1 – 4 from *P. macrocarpa* fruit peels on the mitochondrial membrane potential of *T. cruzi* trypomastigotes. Parasites were treated with the mixture of compounds **1 – 4** for 1 and 2 hours, using JC-1 dye (excitation and emission wavelengths of 488 nm and 530/574 nm, respectively). Parasites treated with CCCP and untreated parasites were the positive (C+) and negative (C-) controls, respectively. A representative assay is shown. ***p< 0.0002

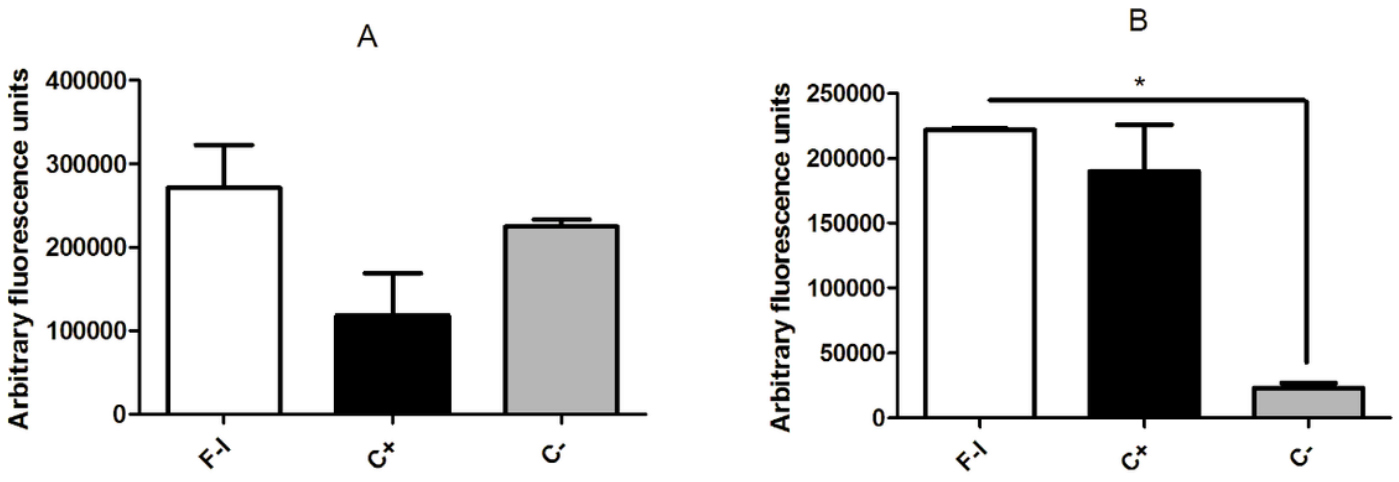


Figure 6

Effect of the mixture of compounds 1 – 4 from P. macrocarpa fruit peels on the levels of reactive oxygen species in T. cruzi trypomastigotes. H_2DCFDA dye (excitation and emission wavelengths of 485 nm and 520 nm, respectively) was used in parasites treated with the mixture of compounds **1 – 4** for 1 and 2 h and the fluorescence was measured. Positive control (C+) was 10 mM azide and untreated T. cruzi was the negative control (C-).*p<0.01

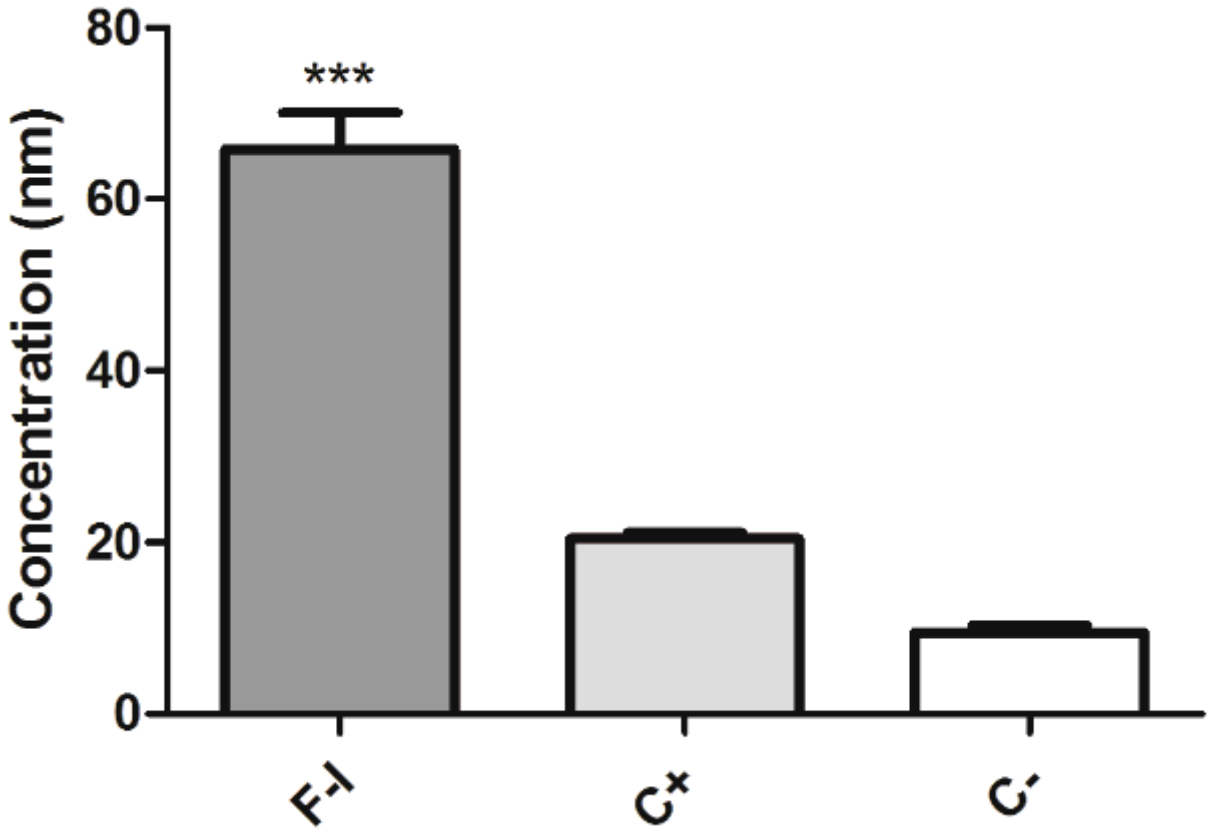


Figure 7

Evaluation of the ATP levels of T. cruzi trypomastigotes after treatment with the mixture of compounds 1 – 4 from P. macrocarpa fruit peels.ATP concentration was measured in a luminometer after 1 h parasite incubation with the mixture of compounds **1 – 4**. Negative (C-) and positive (C+) control were untreated parasites and trypomastigotes treated with 100 µM CCCP, respectively. ***p<0.0001

Supplementary Files

This is a list of supplementary files associated with this preprint. Click to download.

- SUPPORTINGMATERIAL.docx